

Magnetic, resonant, and optical properties of the amorphous magnet $\text{Bi}_2\text{Fe}_4\text{O}_9$

G. A. Petrakovskii, K. A. Sablina, V. E. Volkov, Yu. M. Fedorov, I. M. Stolovitskil, V. I. Chechernikov, and V. L. Yakovenko

Physics Institute, Siberian Division, USSR Academy of Sciences

(Submitted 3 January 1983)

Zh. Eksp. Teor. Fiz. **85**, 592–601 (August 1983)

The magnetic, optical, and resonant properties of amorphous $\text{Bi}_2\text{Fe}_4\text{O}_9$ are measured to determine the effect of amorphization on its magnetic state. It is found that the transition of the antiferromagnetic crystal $\text{Bi}_2\text{Fe}_4\text{O}_9$ to the amorphous state is accompanied by an increase of the magnetic phase transition temperature and by appearance of an uncompensated magnetic moment.

PACS numbers: 75.30.Kz, 75.50.Kj, 75.50.Ee, 78.20. — e

1. INTRODUCTION

Transformation of crystalline matter into the amorphous state alters radically its atomic structure, and this can lead in turn to a complete rearrangement of the magnetic structure and to a drastic change of the magnetic properties.¹ This situation is particularly strongly pronounced in amorphization of compounds with few-dimensional magnetic structure. Naturally, a strong influence of amorphization on the magnetic structure of matter should also be expected in all cases when the arrangement of the atomic structure changes substantially the magnitude and character of the exchange interactions.

As reported by us earlier,² transformation of the antiferromagnetic crystal $\text{Bi}_2\text{Fe}_4\text{O}_9$ into the amorphous state is accompanied by a drastic increase of the magnetic phase transition temperature (by more than two times) and by the onset of an uncompensated macroscopic magnetic moment. We present here the results of a comprehensive investigation of the magnetic, resonant, and optical properties of the amorphous magnet $\text{Bi}_2\text{Fe}_4\text{O}_9$, with an aim at explaining the previously observed effects.

2. SAMPLE PREPARATION

The crystal $\text{Bi}_2\text{Fe}_4\text{O}_9$ has an orthorhombic structure (space group D_{2h}^9) with unit-cell parameters $a = 7.950 \text{ \AA}$, $b = 8.428 \text{ \AA}$, $c = 6.005 \text{ \AA}$.^{3,4} The architectural base of the structure⁵ consists of columns of oxygen octahedra with their edges joined. Between the octahedral columns are connecting links, each consisting of two oxygen tetrahedra. There is thus a single frame of O^{2-} ions. The unit cell contains four octahedra and four tetrahedra. The Fe^{3+} ions in the $\text{Bi}_2\text{Fe}_4\text{O}_9$ lattice are equally distributed among the octahedral and tetrahedral positions. Magnetically, $\text{Bi}_2\text{Fe}_4\text{O}_9$ is a layered collinear antiferromagnet with a Néel temperature $T_N = 265 \text{ K}$.^{4,5} The magnetic moment of the Fe^{3+} ions is $4.95 \mu_B$ (the effective moment equals $5.87 \mu_B$).

We synthesized polycrystalline $\text{Bi}_2\text{Fe}_4\text{O}_9$ samples by the standard ceramic technology. Batches of the oxides Fe_2O_3 and Ni_2O_3 of pure-for-analysis grade, in stoichiometric ratio, were around mixed, and pressed into pellets. The solid-phase reaction lasted 13 hours at 1020 K. An x-ray structure analysis confirmed that the samples were single-phase. A differential thermal analysis (DTA) has revealed the presence of polymorphic transitions at 730, 1040, 1150, and 1180 K; these were observed also in Ref. 6.

The amorphous $\text{Bi}_2\text{Fe}_4\text{O}_9$ was obtained using a catapult oven that made it possible to quench the melt at a rate 10^6 deg/sec. The initial material was melted at 1570 K with a molybdenum-disilicide annular heater. The melt was catapulted into the inner surface of a copper cylinder rotating at $\sim 14\,000$ rpm. Prior to each experiment the working surface of the cylinder was polished to remove the oxide film. The product of the amorphization of $\text{Bi}_2\text{Fe}_4\text{O}_9$ were bright bent plates and black flakes. The x-ray pattern of the quenched molten $\text{Bi}_2\text{Fe}_4\text{O}_9$ obtained with the DRON-2 apparatus (Cu $K\alpha$ radiation) reveals weak diffuse scattering and confirms thereby that the substance is amorphous. This is additionally confirmed by DTA data (Fig. 1), according to which the isothermal crystallization of the amorphous $\text{Bi}_2\text{Fe}_4\text{O}_9$ takes place at 920 K. Prior to the crystallization, at $T \approx 820 \text{ K}$, a weak endo-effect is observed and can be attributed to the vitrification temperature T_g . A similar DTA picture was observed for amorphous $\text{Y}_3\text{Fe}_5\text{O}_{12}$.⁷ According to the DTA data the Néel temperature of the amorphous $\text{Bi}_2\text{Fe}_4\text{O}_9$ is $T_N = 623 \text{ K}$.

Heat treatment of amorphous $\text{Bi}_2\text{Fe}_4\text{O}_9$ in air at 670, 770, 870, and 970 K for four hours has shown that crystallization takes place in fact at 920 K. Raising the heat-treatment temperature to 970 K leads to line narrowing on the x-ray pattern. It was also established that heat treatment in air and in oxygen at $T = 570 \text{ K}$ and higher makes the samples transparent in visible light and red in color. The resistivity of amorphous $\text{Bi}_2\text{Fe}_4\text{O}_9$ is $\sim 10^{10} \Omega\text{-cm}$ at 300 K.

3. MAGNETIC PROPERTIES

All the magnetic measurements were made on powders. The magnetization $\sigma(T)$ was measured with pendulum and pulsed magnetometers in fields up to 10 and 225 kOe respec-

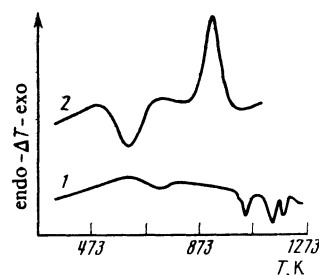


FIG. 1. Thermograms of crystalline (1) and amorphous (2) $\text{Bi}_2\text{Fe}_4\text{O}_9$.

tively and in the temperature range 4.2–1000 K. Figure 2 shows the temperature dependences of $\sigma(T)$ plotted in a 10 kOe field for amorphous and polycrystalline samples. The triangles are the results of measurements on glass heat-treated at $T = 970$ K for 36 h. Since the $\text{Bi}_2\text{Fe}_4\text{O}_9$ crystal undergoes polymorphous transformations when heated to the melting point, it was necessary to check whether the drastic change of the magnetic properties upon amorphization (Fig. 2) were due to fixing of any of the polymorphous phases in the course of quenching. To this end we froze various polymorphous phases by quenching crystalline samples kept for two hours at the temperatures of the corresponding transition. None of these heat treatments changed the initial antiferromagnetic state of the crystal. Nor did the magnetic properties change also after quenching the samples from a temperature close to the melting point. The observed drastic change of the magnetic properties manifests itself thus only when the melt is quenched. We note that according to the data of Fig. 2 the Néel temperature of amorphous $\text{Bi}_2\text{Fe}_4\text{O}_9$ is 620 K.

Figure 3 shows the field dependence of the magnetization of amorphous $\text{Bi}_2\text{Fe}_4\text{O}_9$ at $T = 77$ K, measured in static fields up to 10 kOe, and the same dependence measured in pulsed fields up to 225 kOe at 4.2 K. Measurement of the hysteresis loop at 4.2 K in a field 6 kOe has shown that the coercive force is 300 Oe and decreases by an order of magnitude when the temperature is raised to 77 K. The data of Fig. 3 show that the magnetization reaches saturation $\sigma_0 = 24 \text{ G}\cdot\text{cm}^3/\text{g}$ in a magnetic field close to 130 kOe. This is much lower than the calculated magnetization $\sigma_0 = 142 \text{ G}\cdot\text{cm}^3/\text{g}$ obtained assuming ferromagnetic ordering of the spins of the Fe^{3+} ions in $\text{Bi}_2\text{Fe}_4\text{O}_9$.

Finally, the measured temperature dependence of the magnetic susceptibility χ in a 4 kOe field is shown in Fig. 4. Owing to crystallization we were unable to perform these measurements at $T > 1000$ K. The obtained $\chi(T)$ dependence is typical of ferrimagnets, as is illustrated by the Néel susceptibility curve (Fig. 4), adjusted by using as fit parameters $T_c = 620$ K, an effective magnetic moment $5.57 \mu_B$, and an

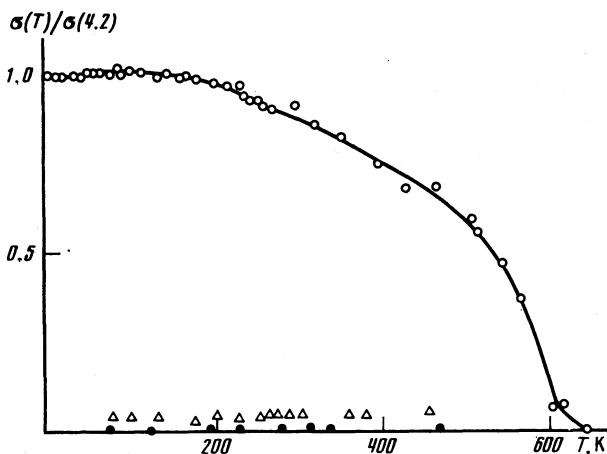


FIG. 2. Temperature dependence of the magnetization in a field 10 kOe: \circ —of the initial glass, \bullet —of polycrystalline sample, \triangle —of glass heat treated at 970 K for 36 h.

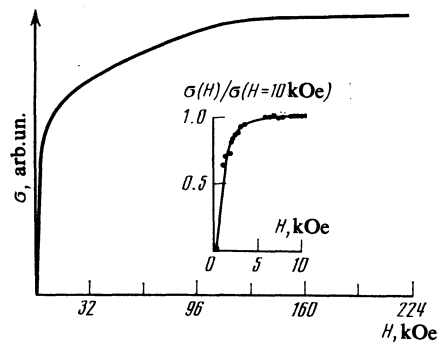


FIG. 3. Dependence of the magnetization of the initial glass $\text{Bi}_2\text{Fe}_4\text{O}_9$ on the field at $T = 4.2$ K.

asymptotic Curie point $\Theta \approx 3000$ K.

Figure 5 shows the values of the magnetization in a 10 kOe field at $T = 4.2$ K and $T = 300$ K for amorphous $\text{Bi}_2\text{Fe}_4\text{O}_9$ samples as functions of the annealing temperature (annealing for 4 hours at each temperature). It can be seen that heat treatment up to 670 K does not change the magnetization. Further increase of the heat-treatment temperature leads to rearrangement of the magnetic structure. The sample annealed at 970 K has a zero spontaneous magnetization.

4. OPTICAL PROPERTIES

The IR spectra of the investigated samples were measured in the range $1600\text{--}400 \text{ cm}^{-1}$ at $T = 300$ K with a Speord 751R spectrometer. The samples for the measurements were made by pressing finely ground powders in a KBr matrix. The most interesting IR region in which intense absorption spectra were observed is shown in Fig. 6. The low-frequency region of the initial-glass spectrum is a superposition of two broad overlapping bands with maxima at 544 and 467 cm^{-1} . The spectra of the glasses heat treated at 670, 770, and 870 K do not differ in practice from the spectrum of the initial glass. Changes in the spectra appear for samples treated above 870 K. Thus, for glass annealed at 970 K the bands are located at 470 and 600 cm^{-1} . In the 800 cm^{-1} region these appears a new relatively weak absorption band. In the sample annealed at 970 K further resolution of the bands is observed. Finally, polycrystalline $\text{Bi}_2\text{Fe}_4\text{O}_9$ shows three pro-

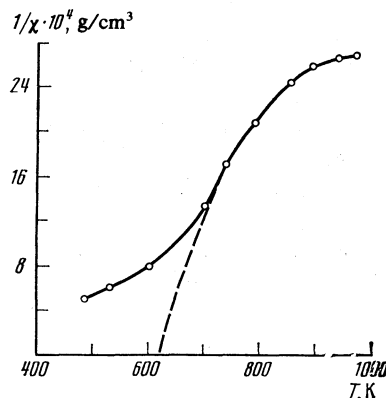


FIG. 4. Dependence of the reciprocal susceptibility on the temperature in a 4 kOe field.

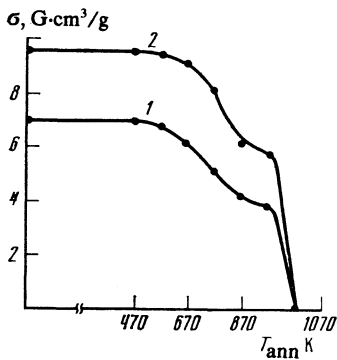


FIG. 5. Dependence of magnetization on the annealing temperature: 1— $T = 300$ K, 2— $T = 4.2$ K.

nounced absorption lines with maxima at 470, 600, and 800 cm^{-1} . To interpret the lines it is useful to bear in mind that in some glassy and crystalline two-component samples, according to the data of Ref. 8, the vibration bands of the octahedrally coordinated ions $\text{Fe}^{3+}(\text{o}) - \text{o}^{2-}$ are located in the frequency region 550–580 cm^{-1} , while those of the tetrahedrally coordinated ions $\text{Fe}^{3+}(\text{t}) - \text{O}^{2-}$ lie in the 625–660 cm^{-1} region. Taking into account this fact and the equality of the number of Fe^{3+} ions in the octahedral and tetrahedral positions of crystalline $\text{Bi}_2\text{Fe}_4\text{O}_9$, we assume that the absorption lines with frequencies 470 and 600 cm^{-1} are due respectively to the vibrations of the Fe^{3+} ion in the octahedral and tetrahedral surrounds. In the glassy sample the line corresponding to the $\text{Fe}^{3+}(\text{t}) - \text{O}^{2-}$ vibrations vanishes and only bands corresponding to $\text{Fe}^{3+}(\text{o}) - \text{O}^{2-}$ vibrations are present. The latter is indirectly confirmed by the fact that in crystalline $\alpha\text{-Fe}_2\text{O}_3$, where only octahedrally coordinated Fe^{3+} ions are present, two absorption bands are likewise observed, with frequencies 560 and 470 cm^{-1} . The narrow

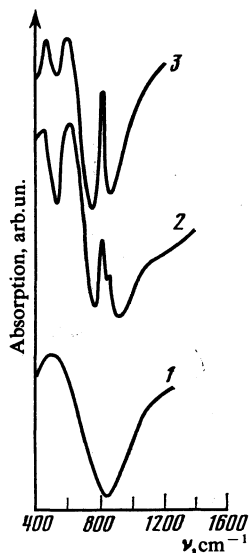


FIG. 6. IR spectra at $T = 300$ K: 1—of initial glass and after heat treatment at 670, 770, and 870 K; 2—of the glass after heat treatment at 970 K; 3—the polycrystalline sample.

800- cm^{-1} absorption band appearing upon crystallization of the amorphous $\text{Bi}_2\text{Fe}_4\text{O}_9$, correlates clearly with the onset of the crystalline phase.

The facts presented give grounds for assuming that when crystalline $\text{Bi}_2\text{Fe}_4\text{O}_9$ is molten and rapidly quenched the atomic structure is so rearranged that the Fe^{3+} ions acquire mainly an octahedral coordination. Iron ions in tetrahedral coordination reappear in the course of the heat treatment.

As already noted, heat treatment of amorphous $\text{Bi}_2\text{Fe}_4\text{O}_9$ in air or in oxygen, starting with ~ 600 K and for several hours, causes the initial black opaque samples to become dark red and transparent in visible light. A similar annealing of the samples all the way to 1000 K in vacuum does not affect the color. It is therefore natural to assume that annealing restores the oxygen stoichiometry that was disturbed in the melt because of the high temperature (~ 1600 K). The shortage of oxygen leads to formation of Fe^{2+} ions whose presence shifts the fundamental absorption edge into the IR region, e.g., in $\text{Y}_3\text{Fe}_5\text{O}_{12}$ single crystals. It is also known that heat treatment of amorphous $\text{Y}_3\text{Fe}_5\text{O}_{12}$ in oxygen makes the samples red and transparent.⁷

We have investigated the optical absorption spectra in the frequency region $(4-18) \times 10^3$ cm^{-1} using an SP-700 spectrophotometer and in the $(18-50) \times 10^3$ cm^{-1} region with a large-aperture MDR-2 monochromator. Figure 7 shows the results for amorphous $\text{Bi}_2\text{Fe}_4\text{O}_9$ samples at different annealing temperatures. It can be seen that the absorption edge of the spectrum shifts gradually to the short-wave side with increasing annealing temperature. On the common absorption wing from the transitions in the UV region one can separate three broad absorption bands that are typical of all the heat treatments. The obtained maxima, viz. 9×10^3 , 14×10^3 , and 24×10^3 cm^{-1} , are typical of Fe^{3+} in a crystal field of cubic symmetry and correspond to the transitions ${}^6A_1 - {}^4T_1$; ${}^6A_1 - {}^4T_2$; ${}^6A_1 - {}^4A_1, {}^4E$ (Ref. 9) from the electronic ground state 6S to the levels, split by the crystal field, of the 4G state. The usual absorption-band broadening of the glassy state is due to the nonequivalent positions of ions with different distortions of the oxygen surround of the iron. With increasing annealing temperature, the absorption bands become more resolved, and the line narrowing of the transitions in the UV region decreases the absorption in the visible part of the band. In view of the proximity of the frequencies of the electronic transitions for the tetrahedrally and octahedrally coordinated Fe^{3+} ions,^{10,11} as well as because of the large absorption-band widths, we were unable to deduce from the spectra of Fig. 7 the local restructuring due to the crystallization of the amorphous $\text{Bi}_2\text{Fe}_4\text{O}_9$.

The broad absorption bands with frequencies 37×10^2 and 45.5×10^2 cm^{-1} recorded for the sample annealed in air for four hours at 770 K can be set in correspondence with the charge-transport process that includes motion of an electron from the oxygen to the iron ion.¹²

Temperature measurements of the optical spectrum have shown that when the temperature of a sample annealed at 770 K is raised the absorption edge is strongly shifted into the long-wave region (Fig. 8), and that the effect is fully reversible when the sample is heated to 770 K.

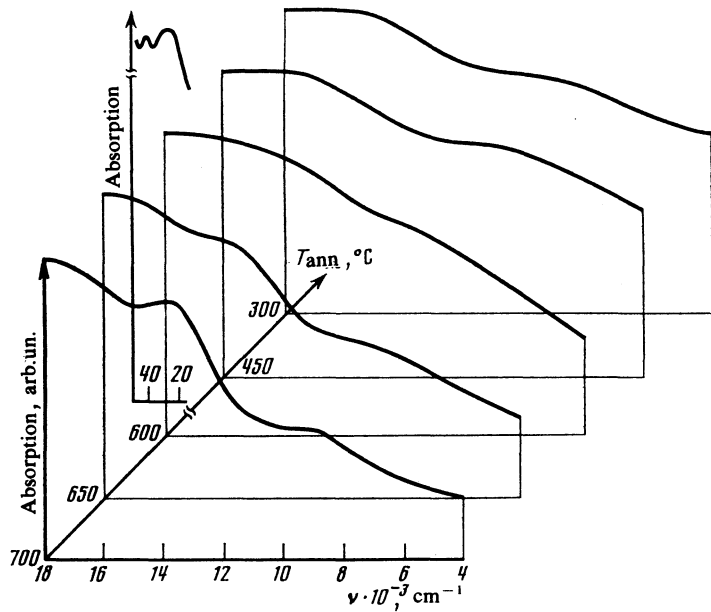


FIG. 7. Optical spectra at $T = 300$ K vs the heat-treatment temperature.

5. RESONANT PROPERTIES

It is known that the state of the spin subsystem of a solid, and particularly the type of the magnetic order, exert a decisive influence on its electron magnetic resonance spectrum. We have investigated the magnetic resonance in amorphous $\text{Bi}_2\text{Fe}_4\text{O}_9$, with an RE-1307 EPR spectrometer at 9100 MHz. The measured temperature dependences of the resonant field and the magnetic-resonance linewidth of amorphous $\text{Bi}_2\text{Fe}_4\text{O}_9$ are shown in Fig. 9. The measurements were made on thin plates 20 μm thick. The resonant field and its relatively strong temperature and orientation dependence are typical for ferromagnetic resonance.

The width ΔH of the resonant absorption line depends strongly on the temperature and on the heat treatment. It can be seen from Fig. 9 that it increases steeply with increasing temperature. Annealing of the initial amorphous $\text{Bi}_2\text{Fe}_4\text{O}_9$ in vacuum at 770 K lowers ΔH insignificantly (by 7%). At the same time, annealing in air or in oxygen decreases the line width to approximately one-half. In view of the results of the optical measurements it is reasonable to suggest that the small decrease of ΔH after vacuum annealing is due to the decreased number of macroscopic inhomogeneities, while the strong decrease of ΔH in the case of annealing in oxygen is due to restoration of the oxygen stoichiometry. The strong growth of ΔH with decreasing temperature is apparently the result of the joint influence of the ionic (due to the Fe^{2+} contamination) and two-magnon (the presence of macroscopic structure defects) ferromagnetic relaxation.¹³ An investigation of the different annealing regimes has shown that the best technological regime that minimizes ΔH (amounting to $\Delta H = 250$ Oe at $T = 300$ K) is annealing for four hours at 770 K in an oxygen atmosphere.

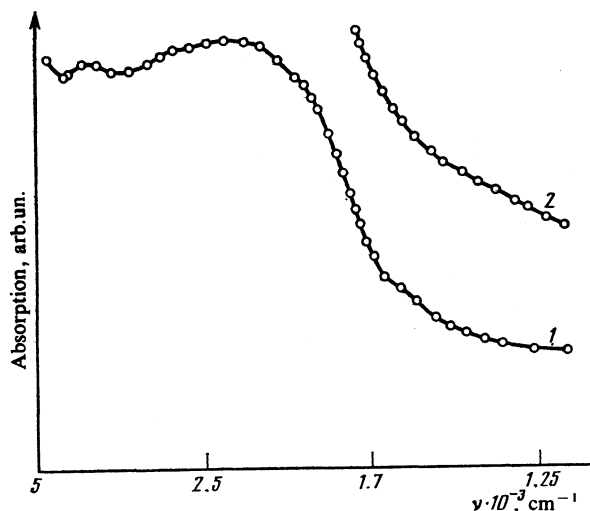


FIG. 8. Optical spectrum of glass after heat treatment at 770 K: 1— $T = 300$ K, 2—770 K.

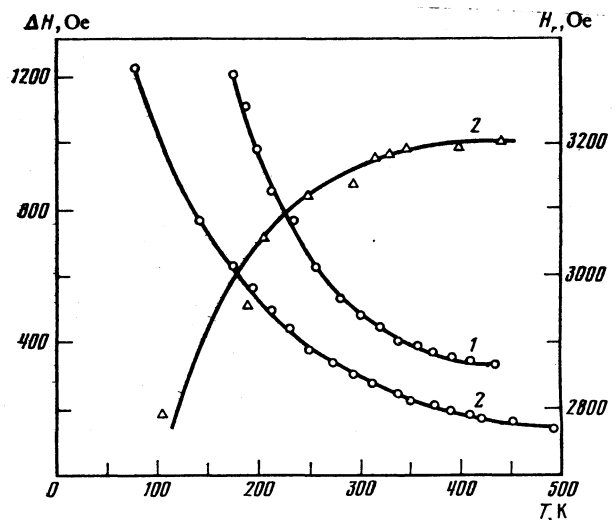


FIG. 9. Temperature dependences of ΔH and H_r for the initial glass (1) and for the glass heat treated at 770 K.

DISCUSSION OF RESULTS

Our results show that rapid quenching of molten $\text{Bi}_2\text{Fe}_4\text{O}_9$ fixes a state with an atomic distribution that differs radically from that of the $\text{Bi}_2\text{Fe}_4\text{O}_9$ crystal. This state is characterized by the absence of long-range atomic order and by a substantial restructuring of the local surround of the iron atoms. The latter manifests itself, in particular, in a vanishing of the tetrahedral coordination of the Fe^{3+} cations. DTA data indicate that the recording state is essentially in thermodynamic disequilibrium and is characterized by considerable heat release. We are consequently justified in assuming that the substance obtained by rapid quenching of the $\text{Bi}_2\text{Fe}_4\text{O}_9$ melt is amorphous.

The amorphization of the initially antiferromagnetic $\text{Bi}_2\text{Fe}_4\text{O}_9$ crystal alters strongly its magnetic properties. The most substantial features of this change are the increase of the magnetic phase-transition temperature from 25 to 620 K and the appearance of spontaneous magnetization. Measurement of the paramagnetic susceptibility shows that the magnetic properties of the amorphous $\text{Bi}_2\text{Fe}_4\text{O}_9$ are produced by the Fe^{3+} ions with elementary magnetic moment per ion $\mu_{\text{eff}} \sim 5.6 \mu_B$. The magnetic structure of the amorphous $\text{Bi}_2\text{Fe}_4\text{O}_9$ at $T < T_N$, according to the measured temperature dependence of the paramagnetic susceptibility and of the magnetization in strong magnetic fields (Figs. 3 and 4), is typical of ferrimagnets. This structure was suggested by us in Ref. 2.

The two-sublattice ferrimagnetic character of the magnetic order of an amorphous magnet can be understood using as an example the lattice model of a magnet with competing exchange interactions. In the region where the ferromagnetism exists, using the elementary coherent-potential approximation,¹ such a magnet is approximated by a translationally invariant single-sublattice ferromagnet with an effective elementary magnetic moment σ . This moment is in the general case smaller than the true magnetic moment σ_0 per site. The real situation, even for the simplest case of a spin $S = 1/2$, should apparently take into account the presence of two spin subsystems corresponding to two directions of their spatial orientation. Numerical calculations by the Monte Carlo methods¹⁴ show that in such systems the distribution function $\rho^{(h)}$ of the local molecular fields h of the form shown in Fig. 10. An essentially distinguishing feature of this function is its asymmetry relative to the origin. The areas under the curves to the right and left of the origin correspond to the normalized magnetizations of the sublattices. The maximum total magnetization of the entire system corresponds to the case of pure ferromagnetic ordering. The

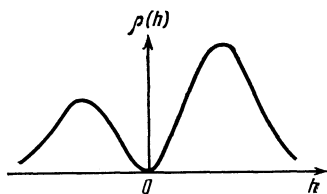


FIG. 10. Distribution function of local molecular fields for an amorphous ferrimagnet.

local magnetic moments $\mu_{A,B}^i$ of the sublattices A and B at the site i is, in the molecular-field approximation,

$$\mu_{A,B}^i = \mu_{A,B}^i(0) B_{S_{A,B}}^i [\mu_{A,B}^i h_{A,B}^i / kT], \quad (1)$$

where $B_S(x)$ is the Brillouin function and $h_{A,B}^i$ are the local molecular fields. The sublattice macroscopic magnetizations $\sigma_{A,B}$ are obtained by configuration averaging of the expression (1)

$$\sigma_{A,B} = \left\langle \frac{\mu_{A,B}^i}{\mu_{A,B}^i(0)} \right\rangle = \left\langle B_{S_{A,B}}^i \left[\frac{\mu_{A,B}^i h_{A,B}^i}{kT} \right] \right\rangle. \quad (2)$$

If the magnetic system is made up of ions of the same sort, Eq. (2) takes the form

$$\sigma_{A,B} = \langle B_S[\mu h_{A,B}^i / kT] \rangle. \quad (3)$$

The total magnetization of the amorphous magnet is

$$\sigma(T) = \tilde{\lambda} \sigma_A(T) - \tilde{\alpha} \sigma_B(T), \quad (4)$$

with $\tilde{\lambda} + \tilde{\alpha} = 1$, where $\tilde{\lambda}$ and $\tilde{\alpha}$ are the average relative numbers of the moments in sublattices A and B . Since the value of (4) is known from experiments, we know consequently that

$$\tilde{\lambda} = \int_0^{h_{\text{max}}} \rho(h) dh, \quad \tilde{\alpha} = \int_{h_{\text{min}}}^0 \rho(h) dh. \quad (5)$$

In particular, in the case of amorphous $\text{Bi}_2\text{Fe}_4\text{O}_9$, according to our experimental data $\tilde{\lambda} = 0.58$ and $\tilde{\alpha} = 0.42$.

It is easy to show that, in the rough molecular-field approximation a system characterized by a molecular-field distribution function of the form shown in Fig. 10 has a Néel paramagnetic susceptibility. Indeed, at temperatures above the Néel point T_N , relation (3) can be simplified:

$$\sigma_{A,B} \approx \frac{S(S+1)}{3S} \frac{\mu \langle h_{A,B}^i \rangle}{kT}. \quad (6)$$

In the presence of an external field H_0 we have

$$\sigma_{A,B} = \frac{C}{T} (H_0 + \langle h_{A,B}^i \rangle), \quad C = \frac{S(S+1)}{3S} \mu. \quad (7)$$

Obviously,

$$h_A^i = \mu \sum_j J_{ij} \sigma_j > 0, \quad h_B^i = \mu \sum_j J_{ij} \sigma_j < 0,$$

where J_{ij} are exchange integrals. We express $h_{A,B}^i$ in the form

$$h_A^i = \mu \sum_{j \in A} \sigma_A^j J_{ij} - \mu \sum_{j \in B} \sigma_B^j J_{ij}, \quad h_B^i = \mu \sum_{j \in B} \sigma_B^j J_{ij} - \mu \sum_{j \in A} \sigma_A^j J_{ij}. \quad (8)$$

We carry out an approximate averaging over the ensemble:

$$h_A = \langle h_A^i \rangle = \mu \sigma_A \left\langle \sum_{j \in A} J_{ij} \right\rangle - \mu \sigma_B \left\langle \sum_{j \in B} J_{ij} \right\rangle, \\ h_B = \langle h_B^i \rangle = \mu \sigma_B \left\langle \sum_{j \in B} J_{ij} \right\rangle - \mu \sigma_A \left\langle \sum_{j \in A} J_{ij} \right\rangle \quad (9)$$

or

$$h_A = \lambda \mu \sigma_A A_{aa} - \alpha \mu \sigma_B A_{ab}, \quad (10)$$

$$h_B = \alpha \mu \sigma_B A_{bb} - \lambda \mu \sigma_A A_{ab},$$

where λ and α are the average numbers of the ions A and B , and A_{ij} are the averaged exchange interactions of the ions of sublattices i and J . It is clear that the system (7) with fields (10) is equivalent to the corresponding equations of the Neel theory of ferrimagnetism,¹⁵ and we have accordingly for the susceptibility

$$\chi^{-1} = \frac{T}{C} + \frac{1}{\chi_0} - \frac{\gamma_0}{T - \Theta}, \quad (11)$$

where

$$\begin{aligned} \chi_0^{-1} &= 2\lambda\alpha A_{ab} - \lambda^2 A_{aa} - \alpha^2 A_{bb}, \\ \gamma_0 &= C\mu\alpha\lambda[\lambda(A_{ab} + A_{aa}) - \alpha(A_{ab} + A_{bb})]^2, \\ \Theta &= \mu C\lambda\alpha(2A_{ab} + A_{aa} + A_{bb}). \end{aligned}$$

This is in fact confirmed by our data on the paramagnetic susceptibility of amorphous $\text{Bi}_2\text{Fe}_4\text{O}_9$.

¹G. A. Petrakovskii, Usp. Fiz. Nauk 134, 305 (1981) [Sov. Phys. Usp. 24, 511 (1981)].

²K. A. Sablina, G. A. Petrakovskii, E. N. Agartanova, and V. P. Piskorskiĭ, Pis'ma Zh. Eksp. Teor. Fiz. 24, 357 (1976) [JETP Lett. 24, 324 (1976)].

³A. G. Tutov, I. E. Myl'nikova, N. N. Parfenova, and S. A. Kizhaev, Fiz. Tverd. Tela (Leningrad) 6, 962 (1964) [Sov. Phys. Solid State 6, 745 (1964)].

⁴N. Shamin, E. Gurewitz, and H. Shaked, Acta Crystallogr. A34, 662 (1978).

⁵V. A. Bokov, S. I. Yushchuk, G. V. Popov, N. N. Parfenova, and A. G. Tutov, Fiz. Tverd. Tela (Leningrad) 13, 1590 (1971) [Sov. Phys. Solid State 13, 1333 (1971)].

⁶L. A. Reznitskiĭ, Izv. AN SSSR, ser. Neorgan. materialy 9, 273 (1973).

⁷E. Gyorgy, K. Nassau, M. Eibshutz, J. Waszczak, C. Wang, and I. Shelton, J. Appl. Phys. 50, 2883 (1979).

⁸K. Marinaga, Y. Siginohara, and T. Yanagase, J. Jpn. Inst. Metals 40, 775 (1976).

⁹D. T. Sviridov, R. K. Sviridova, and Yu. F. Smirnov, Opticheskie spektry ionov perekhodnykh metallov v kristallakh (Optical Spectra of Transition-Metal Ions in Crystals), Nauka, 1976.

¹⁰D. Wood and J. Remeika, J. Appl. Phys. 38, 1038 (1967).

¹¹G. Scott, D. Lacklison, and J. Page, Phys. Rev. 19, 971 (1974).

¹²V. Kh. Khalilov and S. S. Pivovarov, Optical and Spectral Properties of Glasses. Abstracts of 4th All-Union Symposium, Riga, 1977, p. 56.

¹³A. G. Gurevich, Magnitnyi rezonans v ferritakh i antiferromagnetikakh (Magnetic Resonance in Ferrites and Antiferromagnets), Nauka, 1973.

¹⁴G. A. Petrakovskii, E. V. Kuz'min, and S. S. Aplesnin, Fiz. Tverd. Tela (Leningrad) 24, 3298 (1982) [Sov. Phys. Solid State 24, 1872 (1982)].

¹⁵S. V. Vonsovskii, Magnetism, Halsted, 1975.

Translated by J. G. Adashko